ASM Sc. J., 12, Special Issue 4, 2019 for ICSE2018, 97-107

The Modeling and Simulation of MEMS Micropump Model for Insulin Delivery System

Salmah Binti Karman[1], Norhayati Soin[2] and Fatimah Ibrahim[1]

[1]*Department of Biomedical Engineering, Engineering Faculty, University of Malaya, 50603, Malaysia*

[2]*Department of Electrical Engineering, Engineering Faculty, University of Malaya, 50603, Malaysia*

This article presents the simulation study of an electrostatically actuated micropump insulin delivery system for diabetic patients using micro-electromechanical system technology. The structural components of the micropump are a circular bossed silicon membrane. The micropump with a membrane thickness of 8 μm, a boss radius of 600 μm, a boss thickness to membrane thickness ratio (H/h) of 6 and an outlet with 2 ports proved to be the design with the best characteristic flow rate range, about 40 to 1800 nl/min. The final design operates in highly stable pumping rates, 30-190 KHz in the range of safety extra-low voltage (SELV), as low as 42 V. By yielding the nanoliters per minute insulin flow rates, the final micropump design obtained can be integrated to other small devices such as microneedles and others. This integrated micropump can improve the current commercial insulin pump, whereby the insulin treatment process is rendered less invasive, less painful, while at the same time, improving the life quality of diabetic patients.

Keywords: MEMS; micropumps; drug delivery system

I. INTRODUCTION

A. MEMS Micropump Technology

MEMS technology has been used in a number of medical devices and systems, such as micropumps, blood pressure sensors, microneedles, glucose sensors and DNA analyzing systems (Kulinsky & Madou, 2012, Nisar *et al.*, 2008). Micropumps (Mohith *et al.*, 2019, Mahija *et al.*, 2012) are the main part of drug delivery systems that transfer fluids (drugs) from a drug reservoir to the body (tissue or blood vessel). Micropumps are developed in various mechanisms such as piezoelectric, electrostatic, thermopneumatic, pneumatic, shape memory alloy, bimetallic, and via electromagnetic actuation (Mohith *et al.*, 2019). Each actuation principle has its advantages and disadvantages, especially for biomedical applications. Small and high precision micropumps are used for accurate dosing of drug delivery in patients (Shu Dong *et al.* 2019, Shawgo *et al.*, 2002; Borouina *et al.*, 1997).

The electrostatically actuated micropump has the fast response time required in low power consumption insulin micropumps (Nisar *et al.*, 2008) but produces small stroke volume. A center boss structure and a circular shape membrane strengthen the membrane center, thereby prolonging the micropump's lifetime. The bossed structure also helps to stabilize any membrane vibration under high driving frequency (Nambisan & Sharma , 2015, Yih *et al.*, 2005). Furthermore, due to its capability to integrate with microfluidic devices, MEMS electrostatic actuated micropumps can help the implementation of insulin therapy for less invasive therapy which can reduce pain for diabetic patients (Jana & Wadhwani, 2019, Hyunjoo *et al.*, 2018). Presently, diabetic patients depend on conventional drug delivery such as oral tablets consumption or injections using syringes. These conventional methods are invasive, less accurate and have side effects especially for liver function. MEMS insulin delivery technology, on the other hand, offers a better form of insulin therapy that will allow accurate dosing with more efficiency and effectiveness as compared to conventional ways.

The MEMS insulin micropump also has the potentiality to be converged with other devices, such as a glucose sensor and an electrical circuit, to realize the capable function of the intelligent continuous insulin micropump and function like a healthy human pancreas. This device will overcome the weaknesses found in current treatment

*Corresponding author's e-mail: salmah_karman@um.edu.my

techniques, such as an error in insulin injection using syringes which is a common cause of deteriorating blood glucose control. Thus, if this intelligent MEMS insulin delivery is made available, the quality of insulin treatment for diabetic patients will be improved.

In this article, the design of small size, a wide range of flow rate, high pumping stability and low voltage operation MEMS micropump using an electrostatic mechanism for continuous insulin infusion to diabetic patients with body mass ranging from 40 to 70 kg is presented. The micropump model designed by Yih *et al.* (2005) is adopted as the basic design. This basic design model consists of circular bossed silicon membrane micropump, passive flap microvalves, and microchannels.

B. Diabetes Mellitus

Diabetes mellitus is a chronic disease caused by a high blood glucose level that is more than 7.0 mmol/L while fasting. Diabetes mellitus has been classified into several different types, namely Type 1 (insulin-dependent diabetes mellitus; IDDM) and Type 2 (non insulin-dependent diabetes mellitus; NIDDM). Diabetes Type 1 will be detected when the body cannot produce insulin. It usually occurs in children and adults below the age of 40. Diabetes Type 2 typically happens to adults 40 years old and above. It is caused by the decreasing insulin sensitivity. The disease has become the third human killer in the world after cardiovascular disease and cancer. The number of patients is rising every year due to unhealthy lifestyle behaviors such as high-calorie diets and lack of physical activity (Ashrafzadeh & Hamdy, 2019). Reports had claimed that the number of diabetic patients in the world reached 422 million in the year 2014, and 1.6 million death in 2016 (WHO, 2018). International Diabetes Federation reported that until 2017, there were about 3.5 million people in Malaysia detected with diabetes (International Diabetes Federation, 2019). Mortality Country Fact Datasheet 2016 reported by the World Health Organization (WHO) revealed that in 2016, in Malaysia, about 4710 people died due to Diabetes (WHO, 2016).

Patients with diabetes face the risk of infections such as hyperglycemia, macrovascular and microvascular complications (Chew & Leslie, 2006). Tissue damage and cardiovascular diseases such as heart failure and stroke are common diseases caused by these complications. Diabetic patients who take insulin treatment have to plan their meal so that it corresponds to their insulin dosage to avoid hypoglycemia complications. The patients need to monitor their blood glucose level 3 to 4 times a day and need to calculate their carbohydrate intake to cover the insulin taken. The changing of the amount of carbohydrate taken, and the time or the skipping of meals or snacks may all cause the blood glucose level to increase or decrease too much (Ellis, 1934; Jenkins *et al.*, 1994).

Human insulin is a peptide hormone that is involved in both storage and controlled release of energy from food (Curry *et al.*, 1968; Chew & Leslie, 2006). It secretes in two ways: the first is at a basal level where the pancreas delivers a steady, low level of insulin into the bloodstream all day; the second is at bolus level, where large bursts of insulin are released when the blood glucose rises, typically after meals (Diabetes Education Online, 2019). The failure of the body to produce insulin or to respond properly will result in high blood glucose level remaining in blood streams whereby there is a need for external insulin supply in order to avoid the diabetes complication.

There are two ways of using the insulin infusion technique. First, a multi-daily insulin injection (MDII) which uses needles with syringes or insulin pen, while the second is a continuous subcutaneous insulin infusion (CSII) which uses the insulin pump. MDII is a conventional way which requires the patient to take an insulin injection several times a day and more frequently for blood glucose monitoring. Even though this technique is cheap and used by all types of diabetic patients, it brings about a lot of side effects such as great pain and microbial infections which cause discomfort and inconvenience to the patients (Furtado *et al.*, 2006). Unlike MDII, CSII can function like a healthy pancreas better than MDII (MiniMed.Co, 1999). It can deliver insulin directly when needed and not just at fixed times or in localized dosages (Kan, 2005). The insulin pump is an alternative way to prevent the side effects caused by multi-daily insulin injection (MDII) and can reduce the frequency of insulin injections.

The pump such as the one manufactured by Medtronic MiniMed (MiniMed 508) consists of a tiny computer, battery, syringe loaded with very rapid-acting insulin (Boland, 1998) and an infusion set which delivers the amount of insulin to the subcutaneous tissue. The infusion set, which includes a length of tubing and soft cannula at the end, needs to be changed every 2 or 3 days. This pump is adjustable at any time. However, because of its separation from the glucose monitoring device, the patients have to manually set their own basal and bolus

insulin, correction bolus and also to set their routines such as work and play (MiniMed.Co, 1999). The patients also need to operate the insulin pump according to the physician's instruction. In this situation, the user needs the knowledge and effort to operate the insulin pump properly. Only patients who are willing to learn and take on the responsibility would get great benefits (Boland, 1998). The artificial pancreas would be one of the solutions to this limitation. The artificial pancreas will utilize the micropump and glucose sensor as their basic devices. The insulin pump manufactured by Medtronic MiniMed (MiniMed 508) is the best model for the characterization of the insulin small flow rate.

C. Modelling of Fluidic Behavior

By using MiniMed 508, the total daily dosage (TDD) of insulin is divided into basal dose and bolus dose, at 50-50%. The bolus dosage is divided by meals, for example, breakfast bolus; 15%, lunch bolus; 15% and dinner Bolus; 20%. This method requires the patient to fix their carbohydrate intake by depending on the bolus insulin percentage. The initial TDD, k is different for each patient, depends on factors such as age and mass. The insulin pump's beginner needs less insulin, where it will be determined by a doctor, depending on the results of the diagnosis. The range of k used by Medtronic is 0.2 – 0.6 units/kg/day (Minimed.co, 2006), while by University Malaya Medical center (PPUM) is 1 unit/kg/day. The total insulin dosages required by patients with body mass of 40-70 kg in a day are varied, where the smallest TDD (8 units/day) is required by a patient with body mass of 40 kg at the initial TDD, k of 0.2 units/kg/day. The largest TDD (70 units/day) is required by a patient with body mass of 70 kg at the initial TDD k, of 1.0 unit/kg/day. These TDD values will be used for the specification range that will be referred to in the further flow rate study.

The basal insulin flow rate at the smallest and largest TDD values is 28 and 243 nl/min respectively. The flow rate of bolus insulin is determined by using the multi-daily insulin infusion (MDII) in the conventional method, where the bolus insulin will be injected into the patient body using syringe and needles. The time is given for such amount of insulin to be infused into the body varies, depending on the operator of the syringe. For example, the amount of insulin given will enter the body at a high flow rate when the operator operates the syringe in a short time. On the other hand, a lower flow rate of infusion can be obtained to finish the same given amount of insulin by operating the syringe in a longer time. The shorter the given infusion time, the higher the flow rate needs to be. The highest bolus insulin flow rate is 1.4×10^5 nl/min. This value of flow rate is obtained when dinner bolus is infused to the patient with a TDD of 70 units/day in a minute. Due to the analysis above, the range of insulin flow rate that required for artificial pancreas insulin therapy is between 28 to 1.4×10^5 nl/min.

II. METHODOLOGY

The diaphragm is a micropump's structural element which consists of a membrane and boss components such as shown in Figure 1.

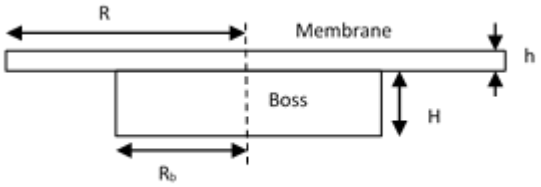

Figure 1. Diaphragm's component (Yih *et al.*, 2005)

As illustrated in Figure 1, h is used to represent the membrane thickness, while H is used to represent the boss thickness. The membrane radius and boss radius is represented by R and Rb respectively. The diaphragm element acts like a sensor, which shows a response when such an input is given. In this study, the response is shown by the diaphragm displacement when the electrostatic actuation is applied. This diaphragm's displacement has a great influence on the development of micropump's models.

The material used for diaphragm structure is silicon (Coventor Manual, 2005), has the density of 2.5e-15 kg/µm3, the dielectric of 11.9, Young's Modulus of 169 GPa and Poisson's ratio of 0.3. The properties of Silicon Nitride (Si_3N_4) and Boron-Doped Phosphosilicate Glass (BPSG) (Coventor Manual, 2005) which are used as insulator components in the fabrication process having the density and Young's Modulus are 2.7e-15 and 2.5e-15 kg/µm3, 222 and 70 GPa respectively. Silicon Nitride and BPSG have the same dielectric value (8.0), while their Poisson's ratios are 0.27 and 0.3 respectively. The density of water (Coventor Manual, 2005) and lispro rapid acting insulin (Eli Lilly and Co., 2005) are 0.998 and 1.003 kg/µm3 respectively, while

their viscosity values are 1.00e-9 and 1.07e-9 mPa.s respectively. The dielectric values of water and lispro rapid acting insulin are 80.2 and 79.6 respectively.

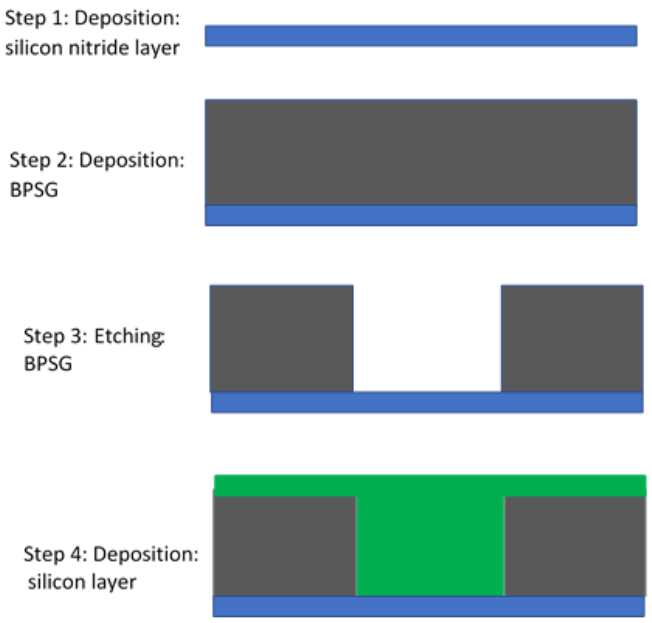

Figure 2. Fabrication process step by step

Table 1. Variation of dimensions of components for FEA analysis

Parametric Analyses	Variable	Variable range
1	Membrane thickness, h	1 µm to 20 µm
2	Boss thickness to membrane thickness ratio, H/h	0 to 20
3	boss radius, R_b	0 to 800 µm

The fabrication steps involve several actions, namely deposition, etching and delete. The fabrication step starts with the deposition of the silicon nitride layer (Si_3N_4) on the silicon substrate, followed by the deposition of Boron-Doped Phosphosilicate Glass (BPSG). The BPSG layer is then shaped into the form of a membrane and boss via the 'etching' process. The dimension of the diaphragm was fixed to 1600 µm. The membrane thickness, boss thickness, and boss dimension were varied according to a wide range of variables shown in Table 1. There are three sets of parametric analyses that will be carried out for FEA since there are three different variables selected.

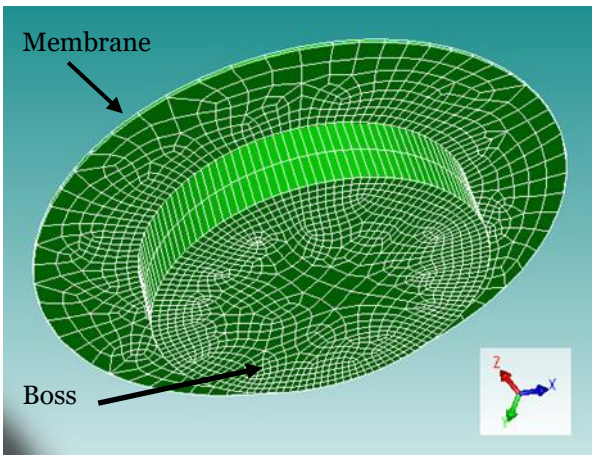

Figure 3. Diaphragm's FEA model of basic design

III. RESULTS AND DISCUSSION

A. Parametric results for diaphragm's structural constants

The diaphragm's sensitivity behavior based on the variation of membrane thickness (h) is presented in a nonlinear trend. By fixing the H/h to 20 and boss radius of 500 µm, as the diaphragm's thickness (h) increased from 1 to 20 µm, the sensitivity decreases in trendline of power curve with equation y=13.044x-1.221 (R^2 = 0.9991). The drastic decrease of sensitivity occurred from point h= 1 µm (sensitivity: 13.82 µm/KPa) to h= 18 µm (sensitivity: 0.41 µm/KPa) . However, there is almost no decrease in the value of sensitivity after the point of h= 18 µm (sensitivity: 0.41 µm/KPa). From the observation of this behavior, it can be seen that the linear portion with a constant value of sensitivity occurs from diaphragm's thickness (h) of 18 to 21 µm, while the nonlinear portion with a variation of sensitivity values occur between 1 to 18 µm.

The nonlinear trend also is shown on the sensitivity behavior of a 10 µm thick diaphragm in varying the boss thickness to membrane thickness ratio (H/h). As the diaphragm is varied from flat to an H/h ratio of 20, the diaphragm with larger H/h ratio shows less sensitivity compared to the smaller one, with huge decreasing of sensitivity occurred before H/h= 16 (Sensitivity value range: 0.0082 to 0.0297 µm/KPa). The sensitivity decrement becomes small as the H/h ratio increases up to 20 (0.0081

μm/KPa).

Again, by maintaining the diaphragm thickness to 10 μm and H/h ratio to 20, the sensitivity of diaphragm decreases as the boss radius is increased up to 800 μm. The highest sensitivity of about 6.9 x10^{-2} μm/kPa, is obtained by the flat diaphragm, while the lowest sensitivity of about 1.42 x 10^{-4} μm/kPa is shown by the diaphragm with a boss radius of 800 μm.

As described by (Di Giovanni, 1982), when the dimensionless ratio Pa4/Eh4 is plotted against the y-h ratio, the linear characteristic is shown for y/h ratio of 0.3 and less. In other words, the curve of y-h ratio can be used to predict the structure stiffness where, the lower the y-h ratio, the stiffer is the diaphragm (Di Giovanni, 1982). From FEA simulation, it can be observed that an effective stiffness characteristic is shown by the diaphragm with a membrane thickness of $\geqslant$ 5 μm, the boss's radius of $\geqslant$ 150 μm and H/h of $\leqslant$ 12, where the y-h ratio is equal or less than 0.3. Table 2 summarizes the variables for effective stiffness and sensitive characteristics. Based on this parametric analysis, the range of variables chosen for the fluidic study of the micropump's structural elements is obtained.

Table 2. Variables with effective stiffness

Variables	**Variables range**
membrane's thickness	5 to 17 μm
boss's radius	150 to 700 μm
boss thickness to membrane thickness ratio, H/h	1 to 12

B. Results of micropump ODE model analysis using MATLAB

Through the analysis conducted using CosolveEM solver in Coventor design software, the capacitance gap of 1 μm gives the largest displacement (2.90 x 10^{-2} (μm)) at safety extra-low voltage (SELV) of 46V. The displacement characteristics have a great influence in determining the performance of stroke volume, where the larger the displacement, the bigger the stroke volume. Clearly, the stroke volume is calculated by multiplying the diaphragm effective area to displacement (Di Giovanni, 1982). The simulation of stroke volume ODE model (Equation 1) using MATLAB software (Yih *et al.*, 2005) resulting in the flow rate characteristics over the parametric variables.

$$\frac{dP_{ch}}{dt} = \frac{I_p(I)\left(\frac{1000}{60}\right)\emptyset_{iv}(P_{iv}) - O_p(I)\left(\frac{1000}{60}\right)\emptyset_{ov}(P_{ov}) + C_{pillar}(2\pi f P_0 \sin(2\pi f t))}{C_{pillar}} \quad (1)$$

Here,

I : insulin to water ratio (0.93)

Ip : inlet port number

Op : outlet port number

Φov : outlet static flow rate

Φiv : inlet static flow rate

Pov : hydrostatic pressure difference (function for outlet flow rate)

Piv : hydrostatic pressure difference (function for inlet flow rate)

Vch : microchamber stroke volume

P : driving pressure

Pch : chamber pressure

Po : amplitude of driving pressure

f : driving frequency

t : time in second

Cpillar : structural diaphragm constant that represents the chamber stroke volume per net pressure denoted by a unit of nl/kPa

Out of simulated variables, only 2 designs obtained the largest flow rate value range, which is up to 1500 nl/min. The 2 designs having a similar membrane thickness of 8 μm and H/h ratio of 6, however, each has a different boss radius. One of the designs utilizes a diaphragm with a boss radius of 500 μm, while the other one has a boss radius of 600 μm at 46 V.

From the simulation performed using MemMech solver in Coventor software, the natural frequencies of design with a boss radius of 500 μm and 600 μm in the smallest mode vibration are about 71 kHz and 81.9 kHz respectively. By varying the frequency between 0 Hz to these natural frequencies, the behavior of flow rate versus frequency for

the two designs is obtained. However, the increase of flow rate at frequencies of over 300 Hz is not significant. Thus, as seen from Figure 10, the flow rate behavior for these 2 designs is only shown for pumping frequencies that vary from 0 to 500 Hz (Yih *et al.*, 2005). These two results are obtained at an applied voltage of 46 V.

As shown in Figure 4, both designs of the micropump exhibit a linear flow rate in a certain frequency range. These designs yield a maximum flow rate of about 1500 nl/min. However, the design with a larger boss radius offers higher stability than the design with a smaller one (Di Giovanni,1982). It can be observed from the graph that the design with a boss radius of 600 µm obtains the maximum flow rate at a pumping frequency of 170 Hz.

The stability characteristics of these two designs also can be found from the image of the top surface of the diaphragm in the displacement state. Figures 5(a) and 5(b) show the image of the diaphragm's top surface displacement for designs with boss radius 500 µm and 600 µm, respectively, at an applied voltage of 46 V.

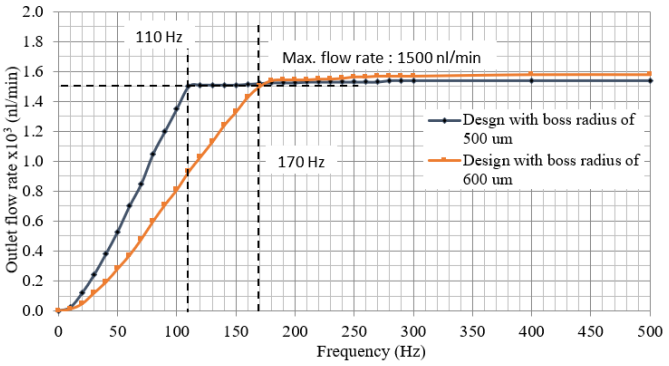

Figure 4. Outlet flow rate versus frequency characteristic for micropump design with boss radius 500 µm and 600 µm at an average applied voltage of 46 V

As a voltage of 46 V is applied to the structures, the design that employs a boss radius of 600 µm shows better stability than the design which uses a boss radius of 500 µm (Di Giovanni, 1982). Instability is detected in the structure with boss radius of 500 µm (Figure 5(a)), where the displacement of the center diaphragm (shown in the red colour) tends to lean towards the diaphragm's edge. Since stability is important to achieve a high-performance micropump, the design with a boss radius of 600 µm is a better choice for the preliminary design.

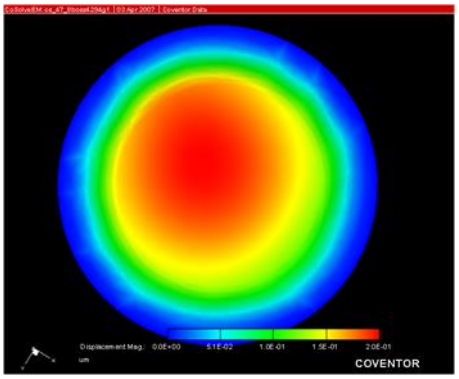

(a)

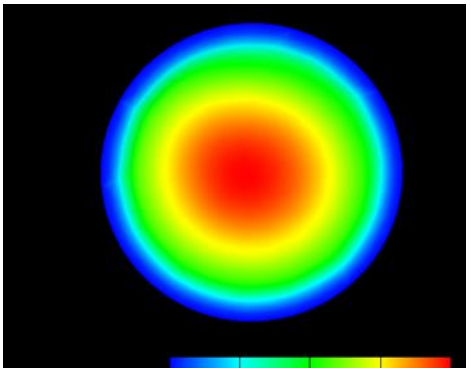

(b)

Figure 5. Image of diaphragm top surface displacement for a boss radius of (a) 500 µm, (b) 600 µm

The design improvement is done in order to reduce the applied voltage as well as to increase the flow rate range. This improvement can be achieved by varying the inlet and outlet port number of the micropump (Zhang & Jullian, 2003; Stoeber & Liepmann, 2005). The dimension of the inlet/outlet port was maintained the same as an original design (Yih *et al.*, 2005). By varying the combination number of inlet and outlet port, the micropump's designs having two inlets-two outlets, two inlets-three outlets and two inlets–four outlets gave the best flow rate range with the maximum value of about 1800 nl/min. Furthermore, choosing the design with two inlet-two outlet ports would be an advantage as it produces a simpler device. The design with two outlets produced pumping performance with a maximum flow rate of 1800 nl/min at 190 Hz. Table 3 compares the characteristics of the micropump before and after outlet port modification.

Table 3. Comparison of the micropump's preliminary and final design at an applied voltage of 46 V

Characteristics	Before modification	After modification
Combination type of inlet and outlet port	2 inlets-1 outlets	2 inlets-2 outlets
Stability, (Hz)	170	190
Maximum flow rate (nl/min)	1500	1800

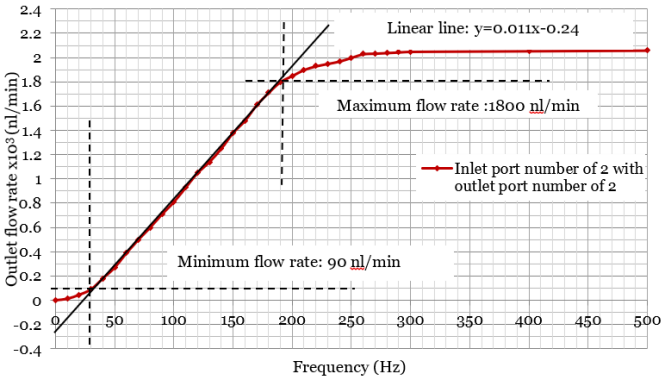

Figure 6. Minimum and maximum flow rate of the micropump design with boss radius 600 µm with modification of 2 inlets-2 outlets port at an average applied voltage of 46 V

The linearity of the curves of the outlet flow rate versus the frequency is determined by using the independent linearity line. The curve that shows zero deviation from the line of independent linearity is assumed to be in the linear region (Di Giovanni, 1982). The frequency and flow rate values at the maximum point of linearity are denoted as "stability point" and "maximum flow rate" respectively. The minimum flow rate is justified within the linear pumping range (Yih *et al.*, 2005; Geipel *et al.*, 2006). As seen from Figure 6, the design resulted in a minimum flow rate of 90 nl/min at the frequency of 30 Hz. The results of the flow rate range characteristic for the modified design with measurements at 38 V, 34 V, 30 V, 24 V, and 18 V are provided in Table 4.

Table 4. Maximum and minimum outlet flow rate characteristics of the modified design at the respectively applied voltage

Average applied Voltage (V)	Stability, (Hz)	Linear pumping range (Hz)	Minimum Flow rate (nl/min)	Maximum Flow rate (nl/min)
46	180	30-190	90	1800
44	190	30-190	50	1800
42	170	30- 170	40	1440
18- 38	-	nonlinear	-	-

As shown in Table 4, a linear pumping rate is produced at operating voltages of 46, 44 and 42 V, whereby the pumping frequencies are between 30 Hz to 190 Hz. Nonlinearity is detected in the curve of flow rate only when the modified design of the micropump operates at 38 V, 34V, 24V and 18 V, where the curve deviates from the linear line. As shown in the column of "maximum flow rate" of Table 5, a maximum flow rate of up to 1800 nl/min is obtained at an applied voltage of 46 V and 44 V. For the minimum flow rate value, the value of 40 nl/min is predicted at the applied voltage of 42 V and 30 Hz pumping frequency. From this study, it is clear that the maximum flow rate value can be obtained by two values of voltage with a difference of about 2 V.

C. Validation

The validation of factors used in this study is analyzed by using the Orthogonal array of L18 of the Taguchi Method. The orthogonal array of L18 is selected since three factors with three "levels" each and one factor with two "levels" are used. Eighteen sets of the simulation are conducted, where different combinations of membrane thickness, H/h ratio, boss radius and combination number of inlet and outlet port are used for each simulation. The range of membrane thickness selected is between 5 µm to 17 µm, H/h ratio is between 1 to 12, and the boss radius is between 150 µm to 700 µm. Table 5 shows the average S/N ratio using Taguchi's orthogonal array of L18.

Table 5. Factors and respective "levels"

Symbols	Factors	factors "level"		
		"level" 1	"level" 2	"level" 3
A	Membrane thickness, h (μm)	5	8	17
B	Boss thickness to membrane thickness ratio, (H/h)	1	6	12
C	Boss radius, R_b (μm)	10	600	700
D	Number of inlet, (Ip) - outlet port ,(Op)	2-1	2-2	-

Table 6. Average of S/N ratio

Symbols	Factors	Average of S/N ratio (dB)			Optimum "level"
		"level" 1	"level" 2	"level" 3	
A	Membrane thickness	32.98	57.59	57.52	A2
B	H/h ratio	46.41	51.81	49.86	B2
C	Boss radius	48.84	50.67	48.58	C2
D	Number of inlet-outlet port	47.55	51.17	-	D2

As shown by Table 6, for factor A(membrane thickness), B(H/h ratio), C(boss radius), and D (number of inlet and outlet port), the highest average S/N ratio is obtained at "level" 2, "level" 2, "level" 2 and "level" 2 respectively for the "the bigger the better". The combination of these factors and "levels", which is denoted as A2B2C2D2, introduces an optimum micropump design that produces the maximum flow rate characteristic, thus enlarge the flow rate range. Using the Taguchi method, the best quality of the final design is proven. A flow rate of 40-1800 nl/min has been achieved by this design.

D. Discussion

Table 7 shows the comparison between the range of flow rate of the final design and the range of flow rate required by the specification of insulin treatment. As described previously, this specification is to be used for insulin treatment on diabetic patients with a body mass of 40 to 70 kg. The specification requires that the minimum flow rate is 28 nl/min and the maximum flow rate is 0.14 ml/min. As indicated in Table 8, the flow rate range of the final design, which is between 40 to 1800 nl/min is valid for this specification. This final design is efficient for the development of a low flow rate micropump, which gives finer control of insulin infusion in its application (Shawgo *et al.*, 2002; Borouina *et al.*, 1997). As reported by Shawgo *et al.*, a finer control of infusion can be obtained by having a flow rate with a range between 1 to 10 μl/min (Shawgo *et al.*, 2002). Borouina et al reported that a flow rate range of 10 to 100 nl/min can also be used in producing a finer control of drug infusion (Borouina *et al.*, 1997). The piezoelectric micropump for drug delivery system in nanoliter per minute flow has been successfully developed with a pumping rate of 4.98 nL per min was obtained at 0.673 kHz at 16V (Johari *et al.*, 2011). The electromagnetic micropump with a matrix-patterned magnetic polymer composite actuator membrane was successfully developed, produced a flow rate of approximately 6.523 nL/min (Said *et al.*, 2017). The thermo pneumatic micropump with a very thin polyimide (Pi) membrane that produced a flow rate range of about 770 pL to 12.5 nL was successfully developed (Hamid *et al.*, 2017). Compared to existing insulin pumps, the micropump with the final design has several differences. The current insulin pump is big in size, operated by a piston mechanism, using a battery with an average voltage of 9 V. This device moderates the insulin infusion flow rate in milliliter per shot, where the minimum and maximum flow rates are about 0.35 ml and 5 ml in a complete shot respectively. The wide range of flow rate that presented by this final design has the advantage to be implemented in insulin therapy as compared to previous design done by Johari *et al.* (2011) and Said *et al.* (2017) because of their single value of flow rate. As in pancreas artificial implementation, the insulin will secret automatically depend on the glucose sensor direction. To ensure the

automatic secretion of insulin can be implemented as good as the healthy pancreas, the single device with a wide range of flow rate is required.

Table 7. Flow rate characteristics

Descriptions	Maximum	Minimum
Flow rate of medical specification (nl/min)	1.4×10^5	28
Flow rate of final design (nl/min)	1.8×10^3	40

In contrast, the final micropump design is smaller in size and uses an electrostatically actuated mechanism by applying a voltage that is varied within the range of 42 to 44 V. Through this final design, the nanoscale insulin flow rate is produced, which will permit this new device to be integrated with other small devices such as microneedles and glucose sensor for less invasive pancreas like insulin therapy.

IV. CONCLUSION

A new design for an electrostatically actuated insulin micropump that offers good range flow rate characteristics as close as conventional insulin therapy with better stability, lower operating voltage and smaller size was developed in this study. The medical specification used in this design development is based on the basal/bolus infusion principle of an existing insulin pump application. The flow rate range presented in this specification is about 28 nl/min to 0.14 ml/min. An ordinary differential equation (ODE) modeling technique is used for designs development since the quasi-static modeling of micropump full system is the approach in this study. The parameters used for the designs are a membrane thickness of 5 µm to 17 µm, diaphragm's boss radius of 150 µm to 700 µm, and boss thickness to membrane thickness ratio (H/h) of 1 to 12. Out of all the variations of designs that have been produced through the parametric study, the design with a membrane thickness of 8 µm, a boss radius of 600 µm, a boss thickness to membrane thickness ratio (H/h) of 6 and an outlet with 2 ports proved to be the design with the best characteristic flow rate range, about 40 to 1800 nl/min. Optimization via the Taguchi Method proved the quality of this design as the best. This final micropump design yields the best flow rate characteristic of about 40 to 1800 nl/min in highly stable pumping rates and can be operated in the range of safety extra-low voltage (SELV), as low as 42 V. By yielding the nanoliters per minute insulin flow rates, the final micropump design obtained can be integrated into other small devices such as microneedles and others. This integrated micropump can improve the current commercial insulin pump, whereby the insulin treatment process is rendered less invasive, less painful, while at the same time, improving the life quality of diabetic patients.

V. ACKNOWLEDGEMENT

This work was supported by the University Malaya PPP grant, BKP088-2017, and RF023A-2018. The special appreciation to MIMOS Sdn Bhd for lending the ConventoreWare license to run this project.

VI. REFEREENCES

Ashrafzadeh, S & Hamdy, O 2019, 'Patient-Driven Diabetes Care of the Future in the Technology Era', *Cell Metabolism*,vol. 29, no. 3, pp. 564-575.

Boland, E 1998, 'Insulin pump therapy : guide for adolescents', *2nd ed. Educational grant from MiniMed*. Model ACC-113 , P/N D9195589-011.

Chew, SL & Leslie, D 2006, *Clinical Endocrinology and Diabetes*, Churchill Livingstone Elsevier, p. 56.

Borouina, T & Bossebœuf, A & Grandchamp, JP 1997, 'Design and simulation of an electrostatic micropump for drug-delivery applications', *Journal of Micromechanics and Microeng*ineering, vol. 7, pp. 186–188.

Diabetes Education Online 2019, *Insulins basics*, University of California, viewed 27 August 2019, < https://dtc.ucsf.edu/types-of-diabetes/type2/treatment-of-type-2-diabetes/medications-and-therapies/type-2-insulin-rx/insulin-basics/>.

Di Giovanni, M 1982, *Flat and Corrugated diaphragm design handbook* CRC Press, New York, USA.

Coventor. Inc. 2005, *Coventor manual version 2005*.

Curry, DL & Bennett, LL & Grodsky, GM 1968, 'Dynamics of Insulin Secretion by the Perfused Rat Pancreas', *Endocrinology*, vol.83, no.3, pp. 572-584.

Eli Lilly and Company 2005, *Insulin Poperties*, *Insulin Lispro Material Safety Data Sheet*, viewed 27 August 2019 <http://ehs.lilly.com/msds/msds_insulin_lispro.pdf >.

Ellis, A 1934, 'Increased carbohydrate tolerance in diabetes following hourly administration of glucose and insulin over long periods' *Quarterly Journal Of Medicine*, vol. 27, pp. 137-53.

Furtado, S & Abramson, D & Simhkay, L & Wobbekind, D & Mathiowitz, E 2006, 'Subcutaneous delivery of insulin loaded poly(fumaric-co-sebacic anhydride) microspheres to type 1 diabetic rats', *Europhean Journal of pharmaceutics and Biopharmaceutics*, vol. 63, pp. 229-236.

Geipel, A & Goldschmidtboeing, F & Jantscheff, P & Esser, N & Massing, U & Woias, P 2008, 'Design of an implantable active microport system for patient specific drug release' *, Biomed Microdevices*, vol.10, no.4, pp.469-78.

Hamid, NA & Majlis, BY & Yunas, J & Syafeeza, AR, Wong, YC & Ibrahim, M 2017, 'A Stack Bonded Thermo-Pneumatic Micro-pump Utilizing, Polyimide Based Actuator Membrane for Biomedical Applications', *Microsystem Technologies*, vol.23, no.9, pp. 4037-4043.

Lee, HJ & Choi, N & Yoon, ES & Cho, IJ 2018, 'MEMS devices for drug delivery', *Advanced Drug Delivery Reviews*, vol. 128, pp. 132-147.

International Diabetes Federation 2019, viewed 22 May 2019 https://www.idf.org/our-network/regions-members/western-pacific/members/108-malaysia.html.

Jana, BA & Wadhwani, AD 2019, 'Microneedle – Future prospect for efficient drug delivery in diabetes management', *Indian Journal of Pharmacology,* vol.51, no.1, pp. 4–10.

Jenkins, DJ & Jenkins, AL & Wolever, TM & Vuksan, V & Rao, AV & Thompson, LU & Josse, RG 1994, 'Low glycemic index: lente carbohydrates and physiological effects of altered food frequency' *American Journal of Clinical Nutrition*, vol.59, no.3 suppl, pp.706S-709S.

Johari, J & Yunas, J & Hamzah, AA & Majlis, BY 2011, 'Piezoelectric Micropump with Nanoliter Per Minute Flow for Drug Delivery Systems', *Sains Malaysiana*, vol.40, no.3, pp. 275–281.

Kan, J & Zhigang, Y & Taijiang, P & Guangming, C 2005, 'Design and test of a high-performance piezoelectric micropump for drug delivery' *Sensor and Actuators A*, vol. 121, pp. 156-161.

Kulinsky, L & Madou, MJ 2012, 'BioMEMs for drug delivery applications', eds B Shekhar & V Abhay in *MEMS for Biomedical Applications*, Woodhead Publishing Series in Biomaterials, pp.218-268.

Mahija, K & Pushpalatha, BG & Jijesh, JJ 2012, 'Mems Based Drug Delivery System Using Micropump', *International Journal of Electronics Signals and Systems (IJESS)*, vol.1 no.4, pp.91-95.

MiniMed.Co 1999, 'Guide to Insulin pump therapy', Mini Med 508 flipchart. *MiniMed professional Education*.

Mohith, S & Karanth, PN & Kulkarni, SM 2019, 'Recent trends in mechanical micropumps and their applications', *A review Mechatronics*, vol.60, pp. 34-55.

Nambisan, RM & Sharma, NN 2015, 'Split-Boss Design For Improved Performance Of MEMS Piezoresistive Pressure Sensor', *International Journal of Electrical, Electronics and Data Communication*, vol.3, no.5, pp. 77-81.

Nisar, A & Afzulpurkar, N & Mahaisavariya, B & Tuantranont A 2008, 'Review: MEMS-based micropumps in drug delivery and biomedical applications', *Sensors and Actuators B*, vol.130, no. 2, pp.917–942.

Said, MM & Yunas, J & Bais, B & Hamzah, AA & Majlis, BY 2017, 'The Design, Fabrication, and Testing of an Electromagnetic Micropump with a Matrix-Patterned Magnetic Polymer Composite Actuator Membrane', *Micromachines*, vol.9, no.13, pp. 1-10.

Shawgo, RS & Grayson, ACR & Li, Y & Cima, MJ 2002, 'Biomems for drug delivery', *Current Opinion in Solid State and Material Science*, vol. 6, no. 4, pp. 329-334.

Stoeber, B & Liepmann, D 2005, 'Arrays of hollow out-of-plane microneedles for drug delivery', *J. Of Microelectromechanical Systems*, vol. 14, no. 3, pp. 472-479.

WHO, Mortality Country Fact Datasheet 2016, viewed 22 May 2019 <https://www.who.int/diabetes/country-profiles/mys_en.pdf?ua=1> .

WHO, Diabetes, 2018, viewed 22 May 2019 <https://www.who.int/news-room/fact-sheets/detail/diabetes>.

Yih, TC & Wei, C & Hammad, B 2005, 'Modelling and characteristic of a nanoliter drug delivery MEMS micropumps with circular bossed membrane', *Nanomedicine : Nanotechnology Biology and medicine* , vol.1, no. 2, pp. 164-175.

Zhang, P & Jullien, GA 2003, 'Micromachined needles for microbiological sample and drug delivery system', *Proceedings of the International Conference on MENS, NANO and Smart Systems, July 20 to July 23, 2003, Banff, Alberta, Canada*.